

Inner Ear Development in Cetaceans

Tara Thean¹, Nikolay Kardjilov², and Robert J. Asher³

¹*(Corresponding author) Department of Zoology, University of Cambridge, Cambridge, UK*

²*Helmholtz-Zentrum Berlin, Berlin, Germany*

³*(Corresponding author) Department of Zoology, University of Cambridge, Cambridge, UK*

INNER EAR DEVELOPMENT, T. THEAN ET AL.

1 Summary

Cetaceans face the challenge of maintaining equilibrium underwater and obtaining sensory input within a dense, low-visibility medium. The cetacean ear represents a key innovation that marked their evolution from terrestrial artiodactyls to among the most fully aquatic mammals in existence. Using micro-CT data and histological data, we document shape and size changes in the cetacean inner ear during ontogeny, and demonstrate that, as a proportion of gestation time, the cetacean inner ear is precocial in its growth compared to that of suid artiodactyls. Cetacean inner ears begin ossifying and reach near-adult dimensions and shape as early as at 32 percent of the gestation period. Our earliest embryos with measurable inner ears (13 percent newborn length) exhibit a flattened cochlea (i.e. smaller distance from cochlear apex to round window) compared to later and adult stages. Inner ears of *Sus scrofa* have neither begun ossifying nor reached near-adult dimensions at 55 percent of the gestation period, but have an adult-like ratio of cochlear diameters to each other, suggesting an adult-like shape. The precocial development of the cetacean inner ear complements previous work demonstrating precocial development of other cetacean anatomical features such as the locomotor muscles to facilitate swimming at the moment of birth.

2 Keywords

inner ear; cochlea; ontogeny; semicircular canals; ossification; cetacean; artiodactyl; suiform

3 Introduction

A central theme in cetacean research is the question of how cetaceans evolved to function entirely and exclusively in water. The fact of cetaceans' obligate aquatic nature is in part a function of what makes them instantly recognizable: their specialized anatomy (see Rose 2006 for review). Though biologists have made considerable progress in investigating cetacean anatomical modifications, many cetacean specialities remain incompletely understood.

29 One such speciality is the cetacean inner ear. Numerous studies have docu-
30 mented cetacean inner ear modifications (see, for example, Gray, 1907; Ketten
31 & Wartzok, 1990; Ketten, 1992; Geisler & Luo, 1996; Lindenlaub & Oelschläger,
32 2000; Solntseva, 2002, 2010). Solntseva (1990) examines peripheral auditory sys-
33 tem development in cetaceans and pinnipeds. Yamato & Pyenson (2015) and
34 Kinkel et al. (2001) provide insight into cetacean middle ear ontogeny, and Solnt-
35 seva (1999) documents how auditory structures form in terrestrial, semi-aquatic,
36 and aquatic species. However, there are still gaps in the current understanding of
37 cetacean inner ear ontogeny and evolution. As Cock (1966) notes, a full under-
38 standing of the genetic differences responsible for the variety of shapes and sizes
39 present in adult animals requires ontogenetic history. Cetacean inner ears are
40 particularly interesting because sound is a crucial means through which cetaceans
41 receive input from their surroundings (Ketten, 1994) and because cetaceans need
42 to move in a three-dimensional environment. Further, the cetacean ear region is
43 able to perform sophisticated functions such as echolocation, particularly in odon-
44 toctetes, and is extremely derived. Derivations of the cetacean inner ear alone
45 are numerous. Among several derived features of the cetacean inner ear, Fleis-
46 cher (1976) describes the low number of turns of cetacean cochleae, the extremely
47 small cetacean semicircular canals (see also Spoor et al. 2002), and the unique
48 odontocete and mysticete modes of cochlear coiling.

49 This paper examines cetacean inner ear ontogeny as it pertains to develop-
50 mental events and growth allometry. We ask when during growth the cetacean
51 inner ear takes on its adult shape and size, and how individual inner ear compo-
52 nents scale with body size during ontogeny. Differences in developmental event
53 timing and relative scaling during growth have contributed to work in mammalian
54 evolution (see Hautier et al. 2012), life histories (see Lu, 2003), and functional mor-
55 phology (see Melin et al. 2005), among other areas. Examinations of ontogenetic
56 allometry in cetaceans are limited. Even studies that have addressed cetacean
57 allometry from an ontogenetic standpoint have often done so only in postnatal
58 specimens (see Clark & Odell, 1999; McLellan et al. 2002) — relatively few have
59 examined foetal specimens as well (see Dunkin et al. 2005; Tsai & Fordyce, 2014;
60 Yamato & Pyenson, 2015). There is relatively little information on how cetacean
61 cranial morphology changes during foetal growth, though the studies on the topic

62 that exist (for example, Klima, 1995; Rauschmann et al. 2006; Armfield et al.
63 2011; Roston et al. 2013) have provided key insights into cetacean evolution and
64 development.

65 Cetaceans are now strongly supported as aquatic artiodactyls — a group of
66 even-toed terrestrial mammals that includes suiforms, tylopods, and ruminants
67 — with hippopotamids as their closest living relatives (see Gatesy et al. 1999;
68 Gingerich et al. 2001; Thewissen et al. 2001; Spaulding et al. 2009 for discussion).
69 Lovell & Harper (2007) endorsed the use of *Sus scrofa* as a model against which to
70 compare cetacean auditory systems, and Kandel & Hullar (2010) used *Bos taurus*
71 to better understand the cetacean vestibular apparatus. As such, we examine inner
72 ear ontogeny in *S. scrofa* as a comparison between terrestrial and obligate aquatic
73 artiodactyls. We seek to observe changes in shape, size, and ossification onset in
74 both whales and a closely related terrestrial artiodactyl (*S. scrofa*). Specifically,
75 we examine whether the timing of ossification onset as well as developmental stage
76 at which the organisms' ears attain adult proportion is conserved or labile between
77 these species. This may shed light on mammalian developmental novelties and the
78 role of the auditory and vestibular apparatus in aquatic life.

79 4 Methods

80 4.1 Three-dimensional data

81 We analyzed 29 unique, unsexed cetacean specimens, including adult petrosals
82 (one specimen each of *Delphinapterus leucas* and *Phocoena phocoena*), a subadult
83 skull (one specimen of *Megaptera novaeangliae*), and embryos or fetuses of up
84 to 40cm in total length (10 specimens of *D. leucas*, four specimens of *Delphinus*
85 *delphis*, one specimen of *Delphinus* sp., two specimens of *P. phocoena*, one speci-
86 men of *Hyperoodon ampullatus*, six specimens of *M. novaeangliae*, one specimen of
87 *Balaenoptera borealis*, and one specimen of *Balaenoptera musculus*, as summarized
88 in Table 1). Our samples for three-dimensional analysis included 20 odontocetes
89 and nine mysticetes. We measured total length as the circumferential (rather than
90 straight) distance between the tip of the rostrum to the tail fluke notch, similar
91 to Yamato & Pyenson (2015), and followed Yamato & Pyenson (2015) in dividing

92 each specimen's total length by previously reported newborn total length measure-
93 ments (see Table 1). We also analyzed four unique, unsexed *S. scrofa* specimens,
94 including an adult skull, a postnatal skull, and two whole fetuses of 23 - 24cm
95 crown rump length (CRL), measured from the top of the head to the tail base.
96 Table 1 provides details of embryonic and foetal specimens.

97 We obtained three-dimensional data for all specimens using micro computed
98 tomography (μ CT) at the Helmholtz-Zentrum Berlin for Materials and Energy
99 (HZB), the American Museum of Natural History (AMNH), and the Departments
100 of Zoology and Engineering, University of Cambridge. We performed the scans
101 with different spatial resolutions varying between 9.8 and 91 μ m depending on the
102 sample size, collecting between 775 and 2316 reconstructed slices for each speci-
103 men. To obtain optimal contrast for the bone tissue we used X-ray energies of up to
104 100kV. We visualized the μ CT data and created three-dimensional reconstructions
105 of inner ear endocasts using the MIMICS Innovation Suite (Materialise's Interac-
106 tive Medical Image Control System) medical imaging software. Due to software
107 limitations we reduced the size of the TIFF format image stacks, first using the Im-
108 ageJ "Binner" plugin (x and y shrink factors of 2, median pixel binning method),
109 and then converting the slices from 16-bit to 8-bit images before importing them
110 into MIMICS. This process resulted in a size reduction from \sim 19-25GB to \sim 1-4GB
111 per stack. In creating three-dimensional reconstructions we used digital segmenta-
112 tion for those scans with fully and densely ossified petrosals as thresholding values
113 were consistently different between tissue boundaries. We used manual segmenta-
114 tion for those scans in which the bony labyrinth was incompletely ossified, and thus
115 whose tissue boundaries were gradients that were sometimes challenging to differ-
116 entiate, to avoid the errors that would likely arise from insufficiently pronounced
117 digital thresholding of boundaries.

118 Following Spoor et al. (2002), we chose the parameters cochlear slant height,
119 first, second, and third (if applicable) cochlear turn diameters, overall cochlea
120 size, and semicircular canal radius of curvature to quantify inner ear anatomy
121 (Figure 1). We also visually inspected each image stack to determine whether or
122 not a specimen's bony labyrinth had ossified. To count the number of cochlear
123 turns in each sample, we approximated the landmarks that Geisler & Luo (1996)
124 used for this purpose. We defined the first landmark as the edge of the round

125 window closest to the “end” of the cochlea in three-dimensional reconstructions,
126 approximating the beginning of the laminar gap that serves as the first landmark in
127 Figure 5 of Geisler & Luo (1996). We took the second landmark to be the cochlear
128 apex, following Geisler & Luo (1996). For those specimens whose bony labyrinths
129 were very incompletely ossified, and thus produced thresholding gradients with
130 noisy three-dimensional reconstructions in MIMICS, we estimated the number of
131 cochlear turns from two-dimensional image stacks in the axial and coronal planes.

132 Cochlear slant height (Spoor et al. 2002) refers to the straight distance between
133 the cochlear apex and the topmost edge (furthest from the apex) of the round
134 window (Gray, 1907; Spoor et al. 2002; see Figure 1a). First, second, and third
135 cochlear turn diameters refer to the largest diameter between the lumen centers of
136 the first, second, and third cochlear turns respectively (see Figure 1b). To ensure
137 consistent and comparable diameters across all specimens, we identified the best fit
138 plane through the anterior semicircular canal (ASC) arc and translated this plane
139 to the parts of the cochlea with the largest cochlear turn diameters, following Spoor
140 (2014, pers. comm.; see Figure 1c). Specimens with cartilaginous bony labyrinths
141 did not possess a clearly visible ASC in μ CT. For these specimens, we estimated
142 analogous planes to the ASC arc-best fit plane based on the position of the round
143 window (when visible), the first and second cochlear turns, and the cochlear apex,
144 following the suggestion of Spoor (2014, pers. comm.). Overall cochlea size refers
145 to the mean of the slant height and the first, second, and third (if applicable)
146 cochlear turn diameters (Spoor et al. 2002). Semicircular canal radius of curvature
147 refers to the average of semicircular canal arc height and width, divided by two
148 (Spoor et al. 2002; Spoor & Thewissen, 2008; Silcox et al. 2009), with arc height
149 and width following the definitions of Spoor & Zonneveld (1995), slightly modified.
150 We measured arc width perpendicular to arc height for all canals (see Figure 1d),
151 and did not account for the angle of the measurements relative to the orientation
152 of the lateral semicircular canal. Some specimens did not have sufficiently ossified
153 bony labyrinths for accurate semicircular canal measurement.

154 We obtained three-dimensional data for 33 adult cetacean specimens and 1
155 adult *S. scrofa* specimen from Spoor et al. (2002). The cetacean specimens in-
156 cluded *Eubalaena glacialis* (2), *Caperea marginalis* (1), *Eschrichtius robustus* (1),
157 *Balaenoptera acutorostralis* (1), *Balaenoptera borealis* (1), *B. musculus* (1), *Bal-*

158 *aenoptera physalis* (1), *M. novaeangliae* (2), *Physeter catodon* (1), *Kogia* sp. (1),
 159 *Berardius bairdii* (1), *Mesoplodon densirostris* (1), *Ziphius cavirostris* (1), *Pla-*
 160 *tanista gangetica* (1), *Inia geoffrensis* (1), *Pontoporia blainvillei* (1), *D. leucas*
 161 (1), *Monodon monoceros* (1), *Delphinus* sp. (2), *Feresa attenuata* (1), *Globi-*
 162 *cephala* sp. (1), *Grampus griseus* (1), *Lagenorhynchus obliquidens* (1), *Orcinus*
 163 *orca* (1), *Stenella* sp. (1), *Tursiops truncatus* (3), *Neophocaena phocaenoides* (1),
 164 and *P. phocoena* (1).

165 4.2 Histological data

166 We analyzed four unique histological series of cetacean embryos from the Univer-
 167 sity of Tübingen (one specimen of *Delphinus* sp., 1200 slices in total, 342 slices
 168 covering one ear, slice distance 20 μ m, Azan-Heidenhain stain), University Museum
 169 of Zoology, Cambridge, or UMZC (one specimen of *Balaenoptera* sp., 1683 slices
 170 in total, 375 slices covering one ear, slice distance 15 μ m, haematoxylin and eosin
 171 stain), and the Zoologisches Museum Berlin, or ZMB (two specimens of *M. no-*
 172 *vaeangliae*, 990 slices in total, 158 slices covering one ear, slice distance unknown,
 173 haematoxylin and eosin stain and 630 slices in total, 220 slices covering one ear,
 174 slice distance unknown, haematoxylin and eosin stain). We analyzed one histologi-
 175 cal series of a *S. scrofa* embryo (868 slices in total, 320 slices covering one ear, slice
 176 distance 40 μ m, Azan-Heidenhain stain) from Tübingen. We photographed histo-
 177 logical slides from Tübingen using a Canon EOS 600D camera, from the UMZC
 178 using a Leica DFC420 camera, and from the ZMB using a Leica DFC490 camera,
 179 and made measurements on those photographs using ImageJ.

180 Three-dimensional reconstructions with μ CT data are possible due to sev-
 181 eral factors, including the consistent inter-slice distance recovered between two-
 182 dimensional reconstructions. Due to the inevitable uncertainties of working with
 183 tissues that have been decalcified, dehydrated, stained, processed on a microtome,
 184 mounted on glass slides, etc., it is not possible with most histological series to be
 185 certain that every slice in a given stack is accounted for. Thus, 100 slices in a
 186 series cut with a thickness of 20 μ a will almost certainly depart at least slightly
 187 from 2mm of anatomy in the original specimen. For these reasons, we create
 188 three-dimensional anatomical reconstructions from μ CT data but not from our

189 histological specimens.

190 Due to the different slicing planes of the histological series, we could not trans-
191 late the ASC arc plane to the part of the cochlea with the largest diameter of the
192 turns. We therefore measured the cochlear diameters of the histological specimens
193 in the planes in which they were originally sliced. For the *S. scrofa* specimen,
194 which was sliced in an axial plane, we estimated the ASC arc plane from the
195 histological slices in which the ASC arc was visible and translated that plane of
196 measurement to the widest parts of the cochlear diameters. We did not measure
197 slant height in the histological specimens because of the specimens' coronal slicing
198 planes and/or the lack of a clearly visible round window in the slices, nor did we
199 measure semicircular canal radii in the histological specimens, as the fact that we
200 could not reslice the histological series according to a best fit plane through each
201 canal meant that there was no way to ensure that we were taking measurements
202 using the correct landmarks on the vestibule and individual canals.

203 We compared foetal inner ear measurements taken from three-dimensional and
204 histological data to those of adults of the same species. We compared our inner
205 ear measurements for *D. delphis* foetal specimens to those of adult *Delphinus* sp.
206 We compared our inner ear measurements for the *Balaenoptera* sp. specimen to
207 the mean inner ear measurements of adult *B. borealis* and *B. musculus*.

208 **4.3 Staging, aging, and body mass**

209 The embryonic and foetal specimens in this study were collected decades ago and
210 thus lack data on individual age. Body length measurements, coupled with mor-
211 phological observations such as external shape, enabled staging and aging of *D.*
212 *delphis* embryos and fetuses according to the Stěrba et al. (2000) classification
213 scheme. We estimated the ages of the *S. scrofa* fetuses using the Ullrey et al.
214 (1965) prediction equation. To enable relative comparisons of foetal cetacean and
215 *S. scrofa* growth with newborn individuals and to estimate how far along the
216 gestation period fetuses were, we used mean gestation period and newborn and
217 adult body length data for various cetacean species and *S. scrofa* from Struthers
218 (1889), Ullrey et al. (1965), Ohsumi (1966), Jefferson et al. (1993), and Stěrba
219 et al. (2000).

220 To enable visual comparison of bony labyrinth shapes between foetal and adult
221 cetaceans as well as foetal and adult *S. scrofa* (Figures 4 and 5), we estimated
222 the body masses of foetal specimens using the equation $W = aL^b$ proposed by
223 Schultz (1938) to predict the weights of large fish and whales, where W is body
224 weight in kilogrammes, L is body length in centimeters, and a and b are constants.
225 Species-specific a and b values from Doidge (1990). For those species whose a and
226 b values Doidge (1990) did not provide we used the values that Schultz (1938)
227 provided to estimate the weights of sharks and whales. We took postnatal *S. scrofa*
228 weight to be the mean weight of the youngest age category (“young pigs before the
229 typical market weight was achieved”, ≥ 5 months old) provided by Mutua et al.
230 (2011). We estimated foetal *S. scrofa* weights using the Pomeroy (1960) prediction
231 equation for estimating foetal weight. We could not estimate the weight of the
232 histological *Delphinus* specimen because only a crown-rump length was provided,
233 or of histological *M. novaeangliae* specimens because no length data were provided.
234 We obtained adult body weight data from Spoor et al. (2002).

235 4.4 Statistical Analysis

236 We analysed body labyrinth shape deviations between foetal and adult cetacean
237 specimens, adult odontocete and adult mysticete specimens, foetal and adult *S.*
238 *scrofa* specimens, and adult cetacean and adult *S. scrofa* specimens by comparing
239 the various groups graphically and/or using Mann-Whitney U tests. We performed
240 all statistical analyses using RStudio 0.97.312.

241 5 Results

242 5.1 Bony labyrinth ossification

243 The bony labyrinth produced enough thresholding contrast to enable three-dimensional
244 reconstruction for some foetal cetacean specimens with body lengths >19 cm and
245 ossified or cartilaginous bony labyrinths, and both foetal *S. scrofa* specimens (Ta-
246 ble 1). None of the bony labyrinths of the histological specimens were ossified; all
247 were cartilaginous. The bony labyrinth was densely ossified in all adult cetacean

248 and *S. scrofa* specimens as well as in the postnatal *S. scrofa* specimen.

249 The largest foetal cetacean specimen in absolute length (27 percent newborn
250 total length, *D. leucas*, ZMB 85708) had a clearly ossified bony labyrinth. Visual
251 inspection via μ CT images showed that this specimen's bony labyrinth was not
252 as densely ossified as the adult *D. leucas* specimen, however. The largest foetal
253 cetacean specimen in percentage of newborn total length (42 percent newborn total
254 length, *Delphinus sp.*, ZMB 85736) also had a clearly ossified bony labyrinth. The
255 largest foetal *S. scrofa* specimen (82 percent newborn total length, UMZC2014.7.1)
256 had a clearly ossified bony labyrinth, though visual inspection via μ CT images
257 showed that its bony labyrinth was also not as densely ossified as the adult *S.*
258 *scrofa* specimen.

259 All *S. scrofa*, cetacean adults, one cetacean subadult specimen, and six cetacean
260 whole fetuses had sufficiently visible bony labyrinths to enable three-dimensional
261 reconstruction of both the semicircular canals and the cochlea. The cetacean
262 specimens were *D. leucas*, *D. delphis*, *Delphinus sp.*, and *P. phocoena* fetuses
263 of between 15 and 42 percent newborn total length and a subadult (26cm) *M.*
264 *novaeangliae* skull. When specimens' bony labyrinths were cartilaginous, the small
265 difference in threshold values between the soft tissues and air as well as the small
266 diameters of the semicircular canal lumina caused the semicircular canals to be
267 indistinguishable from the bony labyrinth's grainy surface. In these cases we could
268 not identify the semicircular canals with confidence. However, our histological data
269 show that they are pre-formed in cartilage at much smaller developmental stages
270 than those of our μ CT-scanned specimens (e.g. *Delphinus sp.* of 14cm CRL).

271 **5.2 Bony labyrinth morphology and measurements**

272 **5.2.1 Cochlea**

273 Foetal *D. leucas* and *P. phocoena* of as little as 13 and 33 percent newborn total
274 length had the same number of cochlear turns as did adults. Comparing foetal
275 and juvenile *D. delphis* and *M. novaeangliae* specimens to adults of those species
276 in the published literature (*D. delphis*, Solntseva, 2010; *M. novaeangliae*, Ketten,
277 1994), showed that foetal and adult specimens of both species had almost the same
278 number of cochlear turns as well.

279 In contrast to the very adult-like cochlear turns among fetuses, cochlear slant
280 heights for foetal cetacean specimens with cochleae that were visible (though not
281 necessarily ossified) in μ CT were smaller than those of adult specimens (Figure 2).
282 The largest foetal cetacean specimen in absolute length (27 percent newborn total
283 length, *D. leucas*, ZMB 85708) had a cochlear slant height of 65 percent of the
284 mean adult slant height. The largest foetal cetacean specimen in percentage of
285 newborn total length (42 percent newborn total length, *Delphinus sp.*, ZMB 85736)
286 exhibited a more adult-like slant height of 79 percent of the mean adult slant height.
287 All foetal cetacean specimens had cochlear slant heights of at least 42 percent of
288 the mean adult cochlear slant height.

289 Cochlear turn diameters in foetal cetacean specimens were smaller than those
290 of adult cochleae. The largest foetal cetacean specimen in absolute length had
291 first and second cochlear turn diameters of 81 and 88 percent the length of the
292 mean adult first and second cochlear turn diameters. The largest foetal cetacean
293 specimen in percentage of newborn total length had first and second cochlear turn
294 diameters of 49 and 42 percent the length of the mean adult first and second
295 cochlear turn diameters. Most foetal cetacean specimens had cochlear turn di-
296 ameters of at least 33 percent of the mean adult size, with the exception of the
297 histological *Delphinus sp.*, *M. novaeangliae*, and *Balaenoptera sp.* specimens.

298 Overall cochlear size of foetal cetacean specimens was between 38 and 75 per-
299 cent that of adult specimens. The largest foetal cetacean specimen in absolute
300 length and the largest foetal cetacean specimen in percentage of newborn total
301 length had overall cochlear sizes of 75 and 59 percent adult size respectively.

302 Both foetal *S. scrofa* specimens (78 and 82 percent of newborn total length) had
303 nearly the same number of cochlear turns (3.25) as did the adult specimen (3.5),
304 while the postnatal *S. scrofa* specimen had the same number of cochlear turns as
305 did the adult specimen. The foetal and postnatal *S. scrofa* specimens had adult-
306 sized cochlear slant heights, and overall cochlea sizes and first, second, and third
307 cochlear turn diameters close to (at least 69 percent of) the mean adult sizes.
308 Meanwhile, the *S. scrofa* histological specimen of 48 percent newborn total length
309 had first and second cochlear turn diameters that were about half the adult size,
310 and a third cochlear turn diameter that was 81 percent the adult size (Table 1).

311 5.2.2 Semicircular canal radius of curvature

312 The semicircular canals were visible in eleven of the foetal and embryonic cetacean
313 specimens in this study — six of the whole fetuses, one subadult specimen, and
314 all four of the histological specimens. Only the posterior semicircular canal was
315 visible in one whole foetal specimen (ZMB 85718), while all three canals were
316 visible in the others. Of the whole fetuses, all had mean semicircular canal
317 radii of at least 51 percent that of the mean adult semicircular canal radii. The
318 largest foetal cetacean specimen in absolute length (27 percent newborn total
319 length, *D. leucas*, ZMB 85708) had a mean semicircular canal radius of 66 percent
320 adult size. The largest foetal cetacean specimen in percentage of newborn total
321 length (42 percent newborn total length, *Delphinus sp.*, ZMB 85736) had a mean
322 semicircular canal radius of 65 percent adult size. The subadult *M. novaengliae*
323 skull (26 percent adult skull length) with a near-adult-sized cochlea had an adult-
324 sized mean semicircular canal radius.

325 Both foetal *S. scrofa* specimens as well as the postnatal specimen had mean
326 semicircular canal radii that were approximately adult-sized.

327 Table 1 provides each specimen's percent adult size for each bony labyrinth
328 variable, while Figure 3 shows these percentages for cochlear variables of the *D.*
329 *leucas* foetal specimens, the species for which we had the greatest number of
330 fetuses with visible bony labyrinths in μ CT.

331 5.2.3 Bony labyrinth shape

332 Neither the ratios of cochlear measurements (slant height, first turn diameter, sec-
333 ond turn diameter) to mean semicircular canal radius of curvature, nor the ratios
334 of these cochlear measurements to each other (e.g., first turn diameter : second
335 turn diameter), were significantly different between adult and foetal odontocete
336 specimens (Figure 4, Figure 5, Table 2). In contrast, the ratio of cochlear first
337 to second turn diameter, the only ratio available for foetal mysticetes, was signifi-
338 cantly different between adult and foetal mysticete specimens ($p < 0.05$, Table 2).
339 We included all available odontocete or mysticete species in each ratio calculation.

340 Ratios between cochlear measurements and mean semicircular canal radius of
341 curvature were significantly different between adult odontocete and adult mys-

342 ticete specimens for all cochlear measurements except for second turn diameter (p
343 < 0.001 for all, Table 2). Ratios between cochlear slant height and second turn
344 diameter and between first and second turn diameter were significantly different
345 between adult odontocete and adult mysticete specimens (p < 0.001 for both ratios,
346 Figure 5, Table 2). The ratio between cochlear slant height and first turn diam-
347 eter was not significantly different between adult odontocete and adult mysticete
348 specimens (Table 2).

349 Sample sizes were insufficient to identify ratio differences between foetal and
350 adult *S. scrofa* via a Mann-Whitney U test, but comparing the foetal and post-
351 natal ratios to adult ratios graphically suggests that ratios are unlikely to be very
352 different between the two groups (Figure 4, Figure 5).

353 6 Discussion

354 This study sought to apply a quantitative lens to how embryonic and foetal inner
355 ear morphologies change during cetacean gestation as well as that of a closely
356 related artiodactyl. We asked both when the form and ossification of the bony
357 labyrinth would emerge during cetacean development, and what the bony labyrinth
358 growth trajectory would look like. Our results provide four major insights:

359 First, bony labyrinth ossification onset has occurred in *D. delphis* at around
360 32 percent of their 280-day intrauterine development period, based on the Stěrba
361 et al. (2000) staging and aging classification of embryos and fetuses. At this stage,
362 the fetuses have attained a body length of at least 24cm, or 29 percent of their
363 approximately 84cm reported newborn total length. Bony labyrinth ossification in
364 *D. leucas* had begun as early as at 15 percent of *D. leucas* newborn total length.

365 Second, cetacean bony labyrinth elements have not achieved full adult size by
366 the time of ossification onset; size maturation continues thereafter. For example,
367 ossified specimens such as AMNH 31735 (*M. novaeangliae*, subadult skull) and
368 ZMB 85708 (*D. leucas*, 27 percent newborn total length) have overall cochlear
369 sizes of 75 percent of their respective adult sizes.

370 Third, bony labyrinth shape, as measured by the ratio of cochlear measure-
371 ments to mean semicircular canal radius of curvature and of cochlear measurements
372 to each other, does not significantly differ between adult and foetal odontocetes in

373 our sample. It significantly differs between adult odontocetes and adult mysticetes,
374 and the ratios between first and second cochlear turn diameters significantly dif-
375 fer between adult and foetal mysticetes. Foetal cochleae demonstrate comparable
376 numbers of turns to those of adult cochleae. They are, however, compressed along
377 the central axis — that is, they have a lower slant height — compared to adult
378 cochleae (Figure 2). Foetal cochlear and semicircular canal arc size reach near-
379 adult proportions early in ontogeny (e.g. at 27 percent newborn total length in *D.*
380 *leucas*).

381 Fourth, the *S. scrofa* bony labyrinth has ossified and reached near-adult pro-
382 portions at 82 percent of its gestation period, when the foetus has attained 78
383 percent of its 29cm newborn total length. The bony labyrinth has not yet ossified
384 or reached adult proportions at 55 percent of the gestation period, which is when
385 the foetus has attained 48 percent of its newborn total length. However, that a
386 foetal cochlea at 55 percent of the gestation period has a nearly equal ratio of first
387 to second cochlear turn diameters to that of an adult *S. scrofa* suggests that the
388 *S. scrofa* bony labyrinth may have attained an adult shape (though not necessar-
389 ily size) at this stage of development. Data for a cetacean bony labyrinth at an
390 equivalent stage of the gestation period were not available for comparison.

391 **6.1 Bony labyrinth ossification and size maturation**

392 As in previous comparative analyses of developmental sequences (e.g. Nunn &
393 Smith, 1998; Smith, 2001; Hautier et al. 2012), we do not assume linearity in
394 development, or that ontogenetic events (such as ossification or attainment of
395 adult proportions in different parts of the skeleton) should happen at the same
396 relative time in different species. Rather, we have collected data to test whether or
397 not they do. Our results suggest that bony labyrinth ossification has begun by the
398 time cetacean fetuses have undergone 32 percent of their intrauterine development
399 period — that is, by ontogenetic Stage 12 of the Stěrba et al. (2000) staging and
400 aging classification of embryos and fetuses. The finding of Moran et al. (2011) that
401 the otic capsule of *Stenella attenuata* is not yet ossified at Stage 23 of Thewissen &
402 Heyning (2007) (which corresponds to Stage 10 and 11 in the Stěrba et al. (2000)
403 classification — stages that actually *succeed* Stage 12) suggests that ossification is

404 unlikely to have occurred prior to Stage 12. In contrast, bony labyrinth ossification
405 does not occur in *S. scrofa* until after 55 percent of gestation has occurred, showing
406 that as a proportion of gestation time, bony labyrinth ossification occurs earlier in
407 cetaceans than in *S. scrofa*. Bony labyrinth ossification also begins proportionally
408 earlier in cetaceans than in humans, whose cochlea and semicircular canals only
409 begin to ossify at 40 and 60 percent of the gestation period respectively (Spector
410 & Ge, 1993). Yamato & Pyenson (2015) note that cetacean ears are the most
411 densely ossified skull bones at roughly 20 and 40 percent of newborn total lengths
412 in mysticetes and odontocetes respectively.

413 Our results also demonstrate that cetacean bony labyrinth size maturation
414 — cochlear slant height, cochlear turn diameter, and semicircular canal radius
415 — continues post-ossification, suggesting a difference between cetacean and hu-
416 man bony labyrinth growth. Jeffery & Spoor (2004) showed that there are few
417 discernible shape changes to the modern human bony labyrinth after otic cap-
418 sule ossification, though Cox & Jeffery (2007) observed minor reorientation of the
419 semicircular canals during growth, and Spector & Ge (1993) note that the human
420 otic capsule achieves adult size before ossification occurs. Human inner ears are
421 therefore closer to adult form than are cetacean inner ears when ossification occurs.

422 Starck (1994) suggests that that ossification limits the rate of post-hatching
423 growth in birds — cartilage facilitates faster growth than does bone, whose histo-
424 genesis involves several differentiation stages. Applying this principle to cetacean
425 inner ear growth, the cetacean inner ear seems to limit its growth before attaining
426 full adult size by ossifying at sub-adult size and then continuing its growth to full
427 adult size under the constraints of ossification, while the human ear grows as car-
428 tilage — presumably at a higher growth rate than that of an ossified cetacean ear
429 — and stops growing when ossified. The ossified foetal *S. scrofa* bony labyrinths
430 we examined were of adult or very near-adult size, suggesting that they may be
431 similar to the modern human bony labyrinth in achieving adult size before ossi-
432 fication occurs. Further study could test this by measuring the bony labyrinth
433 dimensions of newly-ossified *S. scrofa* specimens.

434 The cetacean bony labyrinth ossification onset time — as early as at 32 per-
435 cent of the gestation period — agrees with the suggestion by Bruce (1941) and
436 Hautier et al. (2012) that ossification tends to begin earlier as a proportion of

437 gestation time in species with longer gestation times. As a proportion of gestation
438 time, cetaceans exhibit early ossification onset relative to rodents and terrestrial
439 artiodactyls (e.g. *S. scrofa*). According to Stěrba et al. (2000), the bones of the
440 braincase, face, clavicle, chondrocranium, vertebral arches, ribs, and long limb
441 bones have begun to ossify by Stage 9 (29 percent of the gestation period in *D.*
442 *delphis*, though note that the long bones have ossified by Stage 9 in all species
443 studied by Stěrba et al. (2000) except *D. delphis*). Moran et al. (2011) similarly
444 found that many of the *S. attenuata* skull bones, but not the otic capsule, had be-
445 gun to ossify by Stage 9. With our finding that bony labyrinth ossification occurs
446 at Stage 12 or 32 percent of the gestation period, we can infer that bony labyrinth
447 ossification begins after that of many other skeletal elements, and hence that a
448 large portion of ossification has begun by the time of bony labyrinth ossification
449 onset. This suggests that, like *Loxodonta africana* (see Hautier et al. 2012) and
450 other mammals with prolonged gestation times, many cetacean skeletal elements
451 have experienced ossification onset by the end of the first third of gestation —
452 relatively early compared to mammalian groups such as rodents, in which ossifica-
453 tion onset continues to occur well into the final third of gestation (Hautier et al.,
454 2012).

455 Long gestation periods correlate with precocial development in mammals (Zewel-
456 off & Boyce, 1980; Martin & MacLarnon, 1985; Derrickson, 1992). Cetaceans are
457 unusual among other precocial neonates in having to locomote independently “at
458 the instant of birth” (Dearolf et al. 2000). Developmental traits that likely facil-
459 itate this ability include the adult or near-adult size and shape of the tympanic
460 bulla and periotic in subadult cetaceans (de Buffrenil et al. 2004; Rauschmann
461 et al. 2006; Lancaster et al. 2015) and precocial and positively allometric locomo-
462 tor muscle development (Dearolf et al. 2000; McLellan et al. 2002), among others.
463 Our study finds precocial ossification and size maturation of the bony labyrinth
464 even in the prenatal phase of development. This precocial prenatal ossification and
465 growth of the bony labyrinth may offer protection for other inner ear structures
466 that must be well-developed at birth to enable sensory control of locomotion and
467 detection of acoustic cues. Further work on the prenatal ontogeny of non-skeletal
468 inner ear structures such as the basilar membrane would provide further insight
469 into this possibility.

470 That the *S. scrofa* bony labyrinth has ossified and reached adult proportions
471 at 82 percent, but not 55 percent, of the gestation period suggests that the *S.*
472 *scrofa* bony labyrinth reaches adult-like ossification levels and size later than the
473 cetacean labyrinth, but earlier than that of rodents. Inner ear ossification cen-
474 ters only appear postnatally in *Mesocricetus auratus*, for example (van Arsdel &
475 Hillemann, 1951). Again, this finding corroborates the ossification onset-gestation
476 time link of Bruce (1941) and Hautier et al. (2012), given that *S. scrofa* periotics
477 are among the last cranial elements to ossify (Nunn & Smith 1998). Though our
478 study demonstrates a difference in the timing (as a percentage of gestation) of a
479 developmental event between cetaceans and a closely related artiodactyl, further
480 work that examines a sequence of additional developmental events alongside bony
481 labyrinth ossification in both taxa would be necessary to investigate further de-
482 tails of sequence heterochrony (Smith, 2001; see also Galatius et al. 2006; Galatius,
483 2010; Galatius & Gol'din, 2011 for work on cetacean heterochrony).

484 6.2 Bony labyrinth shape

485 Though limited size maturation continues post-ossification, bony labyrinth shape
486 does not significantly differ between adult and foetal odontocetes. Foetal on-
487 tocetes already exhibit adult-like cochlear coiling. Indeed, Solntseva (1999, 2002)
488 notes that the complete anatomical formation of mammalian cochleae typically
489 occurs before the ear capsule turns cartilaginous. The cetacean cochlea and semi-
490 circular canals also reach near-adult size early in ontogeny (e.g. at 27 percent new-
491 born total length in *D. leucas*). This suggests that the odontocete bony labyrinth
492 achieves adult shape characteristics relatively early in the gestation period. Fur-
493 ther, it shows that a particularly derived cetacean trait — that of relatively small
494 semicircular canals — appears early in ontogeny. The only discernible shape
495 change between adult and foetal odontocetes was that of cochlear slant height,
496 which was significantly different between adult and foetal odontocete species (p
497 < 0.001). Visual inspection of three-dimensional bony labyrinth reconstructions
498 shows the foetal cochleae as flattened compared to the more sharply-pointed organs
499 of adults (Figure 2). Potential functional explanations for this remain unknown.
500 The lengthening of the cochlear spiral along the central axis during development

501 may reflect some frequency range expansion, but without a method for establish-
502 ing cetacean frequency ranges according to cochlear dimensions this possibility
503 remains unexplored.

504 The ratio of first to second cochlear turn diameter was significantly different
505 between adult and foetal mysticetes ($p < 0.05$, note that mysticete adult and foetal
506 ratios were calculated using μ CT and histology respectively due to a lack of visible
507 mysticete foetal bony labyrinths in μ CT data). The less adult-like shape of the
508 foetal mysticete cochlea compared to the foetal odontocete cochlea may reflect the
509 accelerating development that occurs in mysticetes at and after the transition from
510 embryo to foetus (Roston et al. 2013). The histological mysticete specimens we
511 examined all had cartilaginous bony labyrinths, and the *Balaenoptera sp.* spec-
512 imen (the only histological mysticete specimen for which a length measurement
513 was available) had a TL of only 13.7cm, consistent with these specimens' early,
514 embryonic stage of development.

515 Meanwhile, a foetal *S. scrofa* cochlea at 55 percent of the gestation period has
516 nearly equal first to second cochlear turn, first to third cochlear turn, and second
517 to third cochlear turn diameter ratios as an adult *S. scrofa* cochlea, suggesting
518 that the *S. scrofa* bony labyrinth may have attained an adult shape at this stage
519 of development.

520 Bony labyrinth shape was significantly different between adult odontocetes and
521 adult mysticetes for all ratios ($p < 0.001$) except those between cochlear sec-
522 ond turn diameter and mean semicircular canal radius of curvature, and between
523 cochlear slant height and first turn diameter. This result likely relates to the differ-
524 ent modes of coiling of odontocete and mysticete cochleae. Ketten (1992) describes
525 two odontocete modes: Type I cochleae have spirals that resemble “tightly coiled
526 rope”, while Type II cochleae have logarithmic spirals that are more elongated
527 along the central axis. Mysticete cochleae are more elongated along the central
528 axis than those of both odontocete types, and are not coiled in one plane (Fleischer,
529 1976; Ketten, 1992). Fleischer (1976) suggests that a low height to diameter ra-
530 tio of the cochlea (which describes odontocete cochleae more than mysticete ones)
531 helps cetaceans to detect high frequencies. Further, Fleischer (1976) notes that the
532 basal end of some odontocete cochleae curve in a different direction from the rest of
533 the cochlear coiling, a countercurvature that mysticete cochleae can also possess to

534 a smaller extent. Our results suggest that there is a significant difference between
535 the cochlear slant height to second turn diameter ratios of odontocetes and mys-
536 ticetes (the ratio is lower for odontocetes than for mysticetes), but not between the
537 cochlear slant height to first turn diameter ratios of odontocetes and mysticetes.
538 This disparity may arise because of the different definitions of “diameter” between
539 this paper and that of Fleischer (1976), or because of the countercurvature of
540 odontocete cochleae that Fleischer (1976) observed. Text-fig. 1 in Fleischer (1976)
541 and fig. 35.10 in Ketten (1992) provide useful illustrations of the different shapes
542 and modes of coiling between odontocete and mysticete cochleae.

543 **6.3 Inner ear growth allometry and Conclusions**

544 Negative allometry is a common scaling pattern for cetacean skull elements (see
545 Read & Tolley, 1997; McLellan et al. 2002; Spoor et al. 2002). Our results demon-
546 strate that foetal cochlear and semicircular canal size scale with body mass with
547 strong negative allometry, as generally observed for sensory organs throughout
548 vertebrates. *D. leucas* specimens as small as 15 percent of newborn length have
549 cochleae of 68 and 60 percent adult cochlear and semicircular canal size respectively
550 (Table 1). The observed negative allometry of bony labyrinth growth in cetaceans
551 may simply reflect “some form of spatial constraint of otic capsule growth” within
552 the skull (Spoor 2014, pers. comm.).

553 Cetaceans face a unique challenge among mammals in needing to perform a
554 great many life processes entirely in water and being unable to survive outside
555 of the medium. It is thus important to adequately understand the morphological
556 features of the hearing and vestibular apparatus, key systems that make survival
557 possible, in order to better understand the factors that have contributed to their
558 remarkable success in achieving independence from land. We have sought to shed
559 light on the developmental processes of some of these peculiarities, and discuss how
560 they fit into the broader picture of cetacean life history. Inner ear ontogeny is a
561 useful character with which to examine mammalian development, and our results
562 on cetaceans further underscores this order’s uniqueness among mammals.

563 **7 Acknowledgements**

564 We thank the Museum für Naturkunde (Berlin), the University Museum of Zoology
565 (Cambridge), the American Museum of Natural History (New York), the Univer-
566 sity of Cambridge Department of Physiology, Development, and Neuroscience, and
567 Prof. Wolfgang Maier for providing specimens. We thank Wolfgang Maier, Peter
568 Giere, Christiane Funk, Detlef Willborn, and Mathew Lowe for logistical assistance
569 with specimens. Keturah Smithson, Alan Heaver, Morgan Hill, Henry Towbin, and
570 Laura Porro provided technical assistance with μ CT scanning. Wolfgang Maier
571 provided guidance on collecting histological data and feedback on the manuscript.
572 Peter Giere provided guidance on collecting histological data. Fred Spoor, Mary

573 Silcox, and Nicholas Crumpton were valuable sources of advice and information
574 about inner ears. The John Stanley Gardiner Studentship and Queens' College
575 provided financial support for this project. This research also received support
576 from the SYNTHESYS Project (<http://www.synthesys.info/>), which is financed
577 by European Community Research Infrastructure Action under the FP7 Integrat-
578 ing Activities Programme. We thank the editor and reviewers for their comments
579 on the manuscript. The authors declare that they have no conflicts of interest.

580 8 Author Contributions

581 T.T. and R.J.A. conceived the study. N.K., T.T., and R.J.A. performed μ CT scan-
582 ning. T.T. collected histological data, collected measurements from the μ CT and
583 histological data, analyzed and interpreted the data, and wrote the manuscript.
584 R.J.A. supervised the project, assisted with data interpretation, and helped to
585 write the manuscript.

References

- Armfield BA, George JC, Vinyard CJ, Thewissen JGM (2011) Allometric patterns of fetal head growth in mysticetes and odontocetes: Comparison of *Balaena mysticetus* and *Stenella attenuata*. *Mar Mamm Sci* **27**, 819–827.
- Bruce JA (1941) Time and order of appearance of ossification centers and their development in the skull of the rabbit. *Am J Anat* **68**, 41–67.
- Clark ST, Odell DK (1999) Allometric Relationships and Sexual Dimorphism in Captive Killer Whales (*Orcinus orca*). *J Mammal* **80**, 777–785.
- Cock AG (1966) Genetical Aspects of Metrical Growth and Form in Animals. *Q Rev Biol* **41**, 131–190.
- Cox PG, Jeffery N (2007) Morphology of the Mammalian Vestibulo-Ocular Reflex: The Spatial Arrangement of the Human Fetal Semicircular Canals and Extraocular Muscles. *J Morphol* **268**, 878–890.
- de Buffrenil V, Dabin W, Zylberberg L (2004) Histology and growth of the cetacean petro-tympanic bone complex. *J Zool* **262**, 371–381.

- Dearolf JL, McLellan WA, Dillaman RM, Frierson D, Pabst DA (2000) Precocial development of axial locomotor muscle in bottlenose dolphins (*Tursiops truncatus*). *J Morphol* **244**, 203–215.
- Derrickson EM (1992) Comparative Reproductive Strategies of Altricial and Precocial Eutherian Mammals. *Funct Ecol* **6**, 57–65.
- Doidge DW (1990) Age and stage based analysis of the population dynamics of beluga whales, *Delphinapterus leucas*, with particular reference to the northern Quebec population. Ph.D. thesis, McGill University.
- Dunkin RC, McLellan WA, Blum JE, Pabst DA (2005) The ontogenetic changes in the thermal properties of blubber from Atlantic bottlenose dolphin *Tursiops truncatus*. *J Exp Biol* **208**, 1469–1480.
- Fleischer G (1976) Hearing in extinct cetaceans as determined by cochlear structure. *J Paleontol* **50**, 133–152.
- Galatius A (2010) Paedomorphosis in two small species of toothed whales (Odontoceti): how and why? *Biol J Linnean Soc* **99**, 278–295.
- Galatius A, Andersen MER, Haugan B, Langhoff HE, Jespersen Å (2006) Timing of epiphyseal development in the flipper skeleton of the harbour porpoise (*Phocoena phocoena*) as an indicator of paedomorphosis. *Acta Zool* **87**, 77–82.
- Galatius A, Gol'din PE (2011) Geographic variation of skeletal ontogeny and skull shape in the harbour porpoise (*Phocoena phocoena*). *Can J Zool* **89**, 869–879.
- Gatesy J, Milinkovitch M, Waddell V, Stanhope M (1999) Stability of Cladistic Relationships between Cetacea and Higher-Level Artiodactyl Taxa. *Syst Biol* **48**, 6–20.
- Geisler JH, Luo Z (1996) The petrosal and inner ear of *Herpetocetus* sp. (Mammalia: Cetacea) and their implications for the phylogeny and hearing of archaic mysticetes. *J Paleontol* **70**, 1045–1066.
- Gingerich PD, ul Haq M, Zalmout IS, Khan IH, Malkani MS (2001) Origin of whales from early artiodactyls: hands and feet of Eocene Protocetidae from Pakistan. *Science* **293**, 2239–2242.
- Gray AA (1907) *The Labyrinth of Animals*, vol. 1. London: J. & A. Churchill.
- Hautier L, Stansfield FJ, Allen WT, Asher RJ (2012) Skeletal development in the African elephant and ossification timing in placental mammals. *Proc R Soc Lond B Biol Sci* **279**, 2188–2195.

- Jefferson TA, Leatherwood S, Webber MA (1993) *Marine mammals of the world*. Rome: Food & Agriculture Organization of the United Nations.
- Jeffery N, Spoor F (2004) Prenatal growth and development of the modern human labyrinth. *J Anat* **204**, 71–92.
- Kandel M, Hullar TE (2010) The relationship of head movements to semicircular canal size in cetaceans. *J Exp Biol* **213**, 1175–1181.
- Ketten DR (1992) The Marine Mammal Ear: Specializations for Aquatic Audition and Echolocation. In: *The Evolutionary Biology of Hearing*. (eds. Webster DB, Fay RR, Popper AN), pp. 717–750, New York: Springer-Verlag.
- Ketten DR (1994) Functional analyses of whale ears: adaptations for underwater hearing. *IEEE Proc Underwater Acoust* **1**, 264–270.
- Ketten DR, Wartzok D (1990) Three-dimensional reconstructions of the dolphin ear. In: *Sensory Abilities of Cetaceans*. (eds. Thomas JA, Kastelein RA), pp. 81–105, New York: Plenum Press.
- Kinkel MD, Thewissen JGM, Oelschläger HA (2001) Rotation of middle ear ossicles during cetacean development. *J Morphol* **249**, 126–131.
- Klima M (1995) Cetacean phylogeny and systematics based on the morphogenesis of the nasal skull. *Aquat Mammal* **21**, 79–89.
- Lancaster WC, Ary WJ, Krysl P, Cranford TW (2015) Precocial development within the tympanoperiotic complex in cetaceans. *Mar Mamm Sci* **31**, 369–375.
- Lindenlaub T, Oelschläger HA (2000) Preliminary observations on the morphology of the inner ear of the fetal narwhal (*Monodon monoceros*). *Hist Biol* **14**, 47–51.
- Lovell JM, Harper GM (2007) The morphology of the inner ear from the domestic pig (*Sus scrofa*). *J Microsc* **228**, 345–357.
- Lu X (2003) Postnatal growth of skull linear measurements of Cape hare *Lepus capensis* in northern China: an analysis in an adaptive context. *Biol J Linnean Soc* **78**, 343–353.
- Martin RD, MacLarnon AM (1985) Gestation period, neonatal size and maternal investment in placental mammals. *Nature* **313**, 220–223.
- McLellan WA, Koopman HN, Rommel SA, Read AJ, Potter CW, Nicolas JR, et al. (2002) Ontogenetic allometry and body composition of harbour porpoises (*Phocoena phocoena*, L.) from the western North Atlantic. *J Zool* **257**, 457–471.

- Melin AD, Bergmann PJ, Russell AP (2005) Mammalian Postnatal Growth Estimates: The Influence of Weaning on the Choice of a Comparative Metric. *J Mammal* **86**, 1042–1049.
- Moran MM, Nummela S, Thewissen JGM (2011) Development of the skull of the pantropical spotted dolphin (*Stenella attenuata*). *Anat Rec* **294**, 1743–1756.
- Mutua FK, Dewey CE, Arimi SM, Schelling E, Ogara WO (2011) Prediction of live body weight using length and girth measurements for pigs in rural Western Kenya. *J Swine Health Prod* **19**, 26–33.
- Nunn CL, Smith KK (1998) Statistical analyses of developmental sequences: the craniofacial region in marsupial and placental mammals. *Amer Nat* **152**, 82–101.
- Ohsumi S (1966) Allomorphy between body length at sexual maturity and body length at birth in the Cetacea. *J Mamm Soc Japan* **3**, 3–7.
- Pomeroy RW (1960) Infertility and neonatal mortality in the sow III. Neonatal mortality and foetal development. *J Agric Sci* **54**, 31–56.
- Rauschmann MA, Huggenberger S, Kossatz LS, Oelschlger HH (2006) Head morphology in perinatal dolphins: A window into phylogeny and ontogeny. *J Morphol* **267**, 1295–1315.
- Read AJ, Tolley KA (1997) Postnatal growth and allometry of harbour porpoises from the Bay of Fundy. *Can J Zool* **75**, 122–130.
- Rose KD (2006) *The Beginning of the Age of Mammals*. Maryland: Johns Hopkins University Press.
- Roston RA, Lickorish D, Buchholtz EA (2013) Anatomy and age estimation of an early blue whale (*Balaenoptera musculus*) fetus. *Anat Rec* **296**, 709–722.
- Schultz LP (1938) Can the Weight of Whales and Large Fish be Calculated? *J Mammal* **19**, 480–487.
- Silcox MT, Bloch JI, Boyer DM, Godinot M, Ryan TM, Spoor F, et al. (2009) Semicircular canal system in early primates. *J Hum Evol* **56**, 315–327.
- Smith KK (2001) Heterochrony revisited: the evolution of developmental sequences. *Biol J Linn Soc* **73**, 169–186.
- Solntseva GN (1990) Formation of an Adaptive Structure of the Peripheral Part of the Auditory Analyzer in Aquatic, Echo-Locating Mammals During Ontogenesis. In: *Sensory Abilities of Cetaceans* (eds. Thomas JA, Kastelein RA), pp. 363–383, New York: Plenum Press.

- Solntseva GN (1999) Development of the auditory organ in terrestrial, semi-aquatic, and aquatic mammals. *Aquatic Mammals* **25**, 135–148.
- Solntseva GN (2002) Early embryogenesis of the vestibular apparatus in mammals with different ecologies. *Aquatic Mammals* **28**, 159–169.
- Solntseva GN (2010) Morphology of the inner ear of mammals in ontogeny. *Russ J Dev Biol* **41**, 94–110.
- Spaulding M, O’Leary MA, Gatesy J (2009) Relationships of Cetacea (Artiodactyla) among mammals: increased taxon sampling alters interpretations of key fossils and character evolution. *PLoS One* **4**, e7062.
- Spector JG, Ge X (1993) Ossification patterns of the tympanic facial canal in the human fetus and neonate. *Laryngoscope* **103**, 1052–1065.
- Spoor F, Bajpai S, Hussain ST, Kumar K, Thewissen JG (2002) Vestibular evidence for the evolution of aquatic behaviour in early cetaceans. *Nature* **417**, 163–166.
- Spoor F, Thewissen JGM (2008) Comparative and Functional Anatomy of Balance in Aquatic Mammals. In: *Sensory Evolution on the Threshold: Adaptations in Secondarily Aquatic Vertebrates*, pp. 257–284, Berkeley: University of California Press Berkeley, California.
- Spoor F, Zonneveld F (1995) Morphometry of the primate bony labyrinth: a new method based on high-resolution computed tomography. *J Anat* **186**, 271–286.
- Starck JM (1994) Quantitative design of the skeleton in bird hatchlings: Does tissue compartmentalization limit posthatching growth rates? *J Morphol* **222**, 113–131.
- Struthers J (1889) *Memoir on the Anatomy of the Humpback Whale*, Megaptera Logimana. Edinburgh: Maclachlan and Stewart.
- Stěrba O, Klima M, Schildger B (2000) Embryology of Dolphins. Staging and Ageing of Embryos and Fetuses of Some Cetaceans. *Adv Anat Embryol Cell Biol* **157**, 1–133.
- Thewissen JGM, Heyning J (2007) Embryogenesis and development in *Stenella attenuata* and other cetaceans. In: *Reproductive Biology and Phylogeny of Cetacea: Whales, Dolphins, and Porpoises*, pp. 307–329, New Hampshire: Science Publishers.

- Thewissen JGM, Williams EM, Roe LJ, Hussain ST (2001) Skeletons of terrestrial cetaceans and the relationship of whales to artiodactyls. *Nature* **413**, 277–281.
- Tsai C, Fordyce RE (2014) Disparate Heterochronic Processes in Baleen Whale Evolution. *Evol Biol* **41**, 299–307.
- Ullrey DE, Sprague JI, Becker DE, Miller ER (1965) Growth of the swine fetus. *J Anim Sci* **24**, 711–717.
- van Arsdel WC, Hillemann HH (1951) The ossification of the middle and internal ear of the golden hamster (*Cricetus auratus*). *Anat Rec* **109**, 673–689.
- Yamato M, Pyenson ND (2015) Early Development and Orientation of the Acoustic Funnel Provides Insight into the Evolution of Sound Reception Pathways in Cetaceans. *PloS One* **10**, e0118582.
- Zeveloff SI, Boyce MS (1980) Parental investment and mating systems in mammals. *Evolution* **34**, 973–982.

Table 1: Size, cochlear and semicircular canal dimensions relative to those of adult inner ears, and number of cochlear turns for all specimens.

SPECIES	COMMON NAME	SPECIMEN	SIZE (m)	% NEW-BORN TL	OSSIFIED	% ADULT SIZE	TURNS
<i>Delphinapterus leucas</i>	Beluga whale	ZMB 85701	0.25	17	N	C SH D1 D2 D3 R 63 58 64 67 NA NA	2
<i>Delphinapterus leucas</i>	Beluga whale	ZMB 85702	0.20	13	N	65 55 80 50 NA NA	2
<i>Delphinapterus leucas</i>	Beluga whale	ZMB 85703	0.25	17	N	53 51 54 53 NA NA	2
<i>Delphinapterus leucas</i>	Beluga whale	ZMB 85704	0.30	20	N	38 44 33 36 NA NA	2
<i>Delphinapterus leucas</i>	Beluga whale	ZMB 85708	0.40	27	Y	75 65 81 88 NA 66	2
<i>Delphinapterus leucas</i>	Beluga whale	ZMB 85709	0.23	15	Y	56 42 64 68 NA 60	2
<i>Delphinapterus leucas</i>	Beluga whale	ZMB 85710	0.23	15	Y	68 56 75 79 NA NA	2
<i>Delphinapterus leucas</i>	Beluga whale	ZMB 85711	0.30	20	N	NA NA NA NA NA NA	NA
<i>Delphinapterus leucas</i>	Beluga whale	ZMB 85712	0.20	13	N	NA NA NA NA NA NA	NA
<i>Delphinapterus leucas</i>	Beluga whale	ZMB 85714	0.35	23	N	NA NA NA NA NA NA	NA

Table 1: Size, cochlear and semicircular canal dimensions relative to those of adult inner ears, and number of cochlear turns for all specimens.

SPECIES	COMMON NAME	SPECIMEN	SIZE (m)	% NEW-BORN TL	OSSIFIED	% ADULT SIZE	TURNS
<i>Delphinus delphis</i>	Short-beaked common dolphin	ZMB 85720	0.25	30	Y	C SH D1 D2 D3 R 41 50 36 34 NA 53	2
<i>Delphinus delphis</i>	Short-beaked common dolphin	ZMB 4056	0.26	31	N	NA NA NA NA NA NA NA NA NA NA NA NA	NA
<i>Delphinus delphis</i>	Short-beaked common dolphin	ZMB 85721	0.10	12	N	NA NA NA NA NA NA NA NA NA NA NA NA	NA
<i>Delphinus delphis</i>	Short-beaked common dolphin	ZMB 85722	0.06	7	N	NA NA NA NA NA NA NA NA NA NA NA NA	NA
<i>Delphinus</i> sp.	Common dolphin	ZMB 85736	0.35	42	Y	59 79 49 42 NA 65	2
<i>Delphinus</i> sp.	Common dolphin	UT Delphinus1	0.14*	NA	N	NA NA 43 30 NA NA NA NA NA NA NA NA	NA
<i>Phocoena phocoena</i>	Harbour porpoise	ZMB 85717	0.25	33	Y	69 71 71 60 NA 77	1.75
<i>Phocoena phocoena</i>	Harbour porpoise	ZMB 85718	0.19	25	Y	62 59 67 58 NA 51	1.5-2
<i>Hyperoodon ampullatus</i>	Northern bottlenose whale	ZMB 85518	0.19	5	N	NA NA NA NA NA NA NA NA NA NA NA NA	NA
<i>Megaptera vaeangliae</i>	Humpback whale	ZMB 37784	0.25	6	N	NA NA NA NA NA NA NA NA NA NA NA NA	NA

Table 1: Size, cochlear and semicircular canal dimensions relative to those of adult inner ears, and number of cochlear turns for all specimens.

SPECIES	COMMON NAME	SPECIMEN	SIZE (m)	% NEW-BORN TL	OSSIFIED	% ADULT SIZE	TURNS
<i>Megaptera vaeanaliae</i>	Humpback whale	ZMB 85515	0.25	6	N	C SH D1 D2 D3 R NA NA NA NA NA NA NA	NA
<i>Megaptera vaeanaliae</i>	Humpback whale	ZMB 37786	0.35	8	N	NA NA NA NA NA NA NA	NA
<i>Megaptera vaeanaliae</i>	Humpback whale	ZMB 85699	0.04	0.9	N	NA NA NA NA NA NA NA	NA
<i>Megaptera vaeanaliae</i>	Humpback whale	ZMB 37783	0.10	2	N	NA NA NA NA NA NA NA	NA
<i>Megaptera vaeanaliae</i>	Humpback whale	ZMB 85697	0.06	1	N	NA NA NA NA NA NA NA	NA
<i>Megaptera vaeanaliae</i>	Humpback whale	AMNH 31735 (skull)	0.26	26 (% new-born skull length)	Y	75 Ad 67 36 NA Ad	2
<i>Megaptera vaeanaliae</i>	Humpback whale	Megaptera serie 1-21	?	NA	N	NA NA 34 28 NA NA NA	NA
<i>Megaptera vaeanaliae</i>	Humpback whale	Megaptera IX	?	NA	N	NA NA 18 14 NA NA NA	NA
<i>Balaenoptera borealis</i>	Sei whale	UMZC C.17.M	0.31	7	N	NA NA NA NA NA NA NA	NA
<i>Balaenoptera musculus</i>	Blue whale	UMZC C.14.D	0.28	4	N	NA NA NA NA NA NA NA	NA

Table 1: Size, cochlear and semicircular canal dimensions relative to those of adult inner ears, and number of cochlear turns for all specimens.

SPECIES	COMMON NAME	SPECIMEN	SIZE (m)	% NEW-BORN TL	OSSIFIED	% ADULT SIZE	TURNS
<i>Balaenoptera</i> sp.	Rorqual	UMZC Bp1	0.14	2	N	C SH D1 D2 D3 R	NA
<i>Sus scrofa</i>	Wild boar	DPDN 1 (skull)	?	NA	Y	87 Ad 69 90 Ad 99	3.5
<i>Sus scrofa</i>	Wild boar	UMZC 2014.7.1	0.24*	82	Y	86 Ad 77 91 86 99	3.25
<i>Sus scrofa</i>	Wild boar	UMZC 2014.7.2	0.23*	78	Y	86 Ad 78 90 79 96	3.25
<i>Sus scrofa</i>	Wild boar	UT Sus1	0.14*	48	N	NA NA 52 57 81 NA	NA
<i>Delphinapterus leucas</i>	Beluga whale	Delphinapterus C77F (Adult petrosal)	?	NA	Y	Ad Ad Ad Ad NA Ad	2
<i>Phocoena phocoena</i>	Harbour porpoise	Phocoena C80G (Adult petrosal)	?	NA	Y	Ad Ad Ad Ad NA Ad	1.75
<i>Sus scrofa</i>	Wild boar	DPDN 2 (Adult skull)	?	NA	Y	Ad Ad Ad Ad Ad Ad	3.5

TL, total length; C, overall cochlear size; SH, slant height; D1, first turn diameter; D2, second turn diameter; D3, third turn diameter; R, mean semicircular canal radius of curvature; NA = no measurement due to insufficient bony labyrinth ossification or measurement not taken (e.g. D3 in cetaceans with only two cochlear turns); Ad = Adult; Y = Yes; N = No. "Size" column refers to total length (TL) except where specimen is a skull, adult petrosal,

or size value comes with an asterisks, which denotes crown-rump length. Only a crown-rump length was available for some histological specimens. % newborn TL for *Balaenoptera sp.* taken as percentage of average newborn TL of *B. musculus* and *B. borealis*, since these were the two *Balaenoptera* species included in our dataset. % newborn TL of *D. delphis* calculated as percentage of newborn *Delphinus sp.* TL.

Table 2: P-values of Mann-Whitney U tests of ratios between cochlear parameters and mean semicircular canal radius of curvature, and cochlear parameters and each other.

Data Group	P-values									
	SH : R	D1 : R	D2 : R	C : R	SH : D1	SH : D2	D1 : D2			
Adult odontocetes vs foetal odontocetes	0.71	0.98	0.93	1.00	0.72	0.50	0.08			
Adult mysticetes vs foetal mysticetes	NA	NA	NA	NA	NA	NA	0.0020			
Adult odontocetes vs adult mysticetes	2.7e-05	5.02e-05	0.89	0.00063	0.72	2.4e-05	5.5e-08			

Abbreviations as for Table 1.

9 Figure Legends

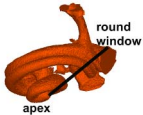
Figure 1: (a) Measurement of cochlear slant height in an adult *D. leucas* specimen, taken as the distance between the cochlear apex and the topmost edge (furthest from the apex) of the round window (Gray, 1907; Spoor et al. 2002). (b) First and second turn diameter measurements in an adult *D. leucas* specimen in the plane of the ASC arc. Blue line: first turn; red line: second turn. (c) Best fit plane through the ASC arc in an adult *D. leucas* specimen, represented by black line. We translated this best fit plane to the part of the cochlea with the largest diameter of the first and second turns to measure the first and second cochlear turn diameter. Modeled from instructive diagrams by Fred Spoor. (d) Measurement of semicircular canal height and width, as defined by Spoor & Zonneveld (1995). The average of these measurements is then divided by two to obtain the semicircular canal radius of curvature.

Figure 2: Three-dimensional reconstructions of *D. leucas* bony labyrinths over ontogeny: (a) 23cm foetus (b) 40cm foetus (c) Adult. The reconstructions demonstrate the elongation of the *D. leucas* cochlea along its central axis — that is, the increase in cochlear slant height, or apex-round window distance — over ontogeny. Bony labyrinth coiling remains consistent. We removed stray pixels in Figure 6 (a) and (b), and flipped both images so that they faced the same direction as Figure 6 (c) for ease of comparison.

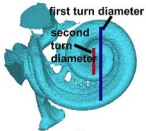
Figure 3: Measurements of cochlear slant height, first and second turn diameters, overall cochlear size, and semicircular canal radius of curvature in six foetal *D. leucas* expressed as percentages of mean adult size. Percentages of newborn total length based on calf data given in Ohsumi (1966) are as follows: ZMB 85709 (15%, blue), ZMB 85710 (15%, pink), ZMB 85701 (17%, orange), ZMB 85703, (17%, ochre), ZMB 85704 (20%, green), ZMB 85708 (27%, turquoise).

Figure 4: Bivariate plots of ratios of cochlear parameters to mean semicircular canal radius of curvature onto logarithmically transformed body mass for adult odontocetes, adult mysticetes, foetal odontocetes, adult *S. scrofa*, and foetal *S. scrofa*. Data points: red, adult odontocetes; blue, adult mysticetes; green, foetal odontocetes; orange, adult *S. scrofa*; purple, foetal *S. scrofa*. Abbreviations: R, mean semicircular canal radius of curvature.

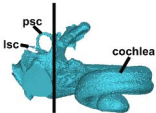
Figure 5: Bivariate plots of ratios of cochlear parameters to each other onto logarithmically transformed body mass for adult odontocetes, adult mysticetes, foetal odontocetes, foetal mysticetes, adult *S. scrofa*, and foetal *S. scrofa*. Data points: red, adult odontocetes; blue, adult mysticetes; green, foetal odontocetes; black, foetal mysticetes; orange, adult *S. scrofa*; purple, foetal *S. scrofa*.



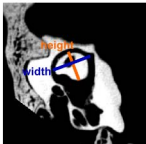
a



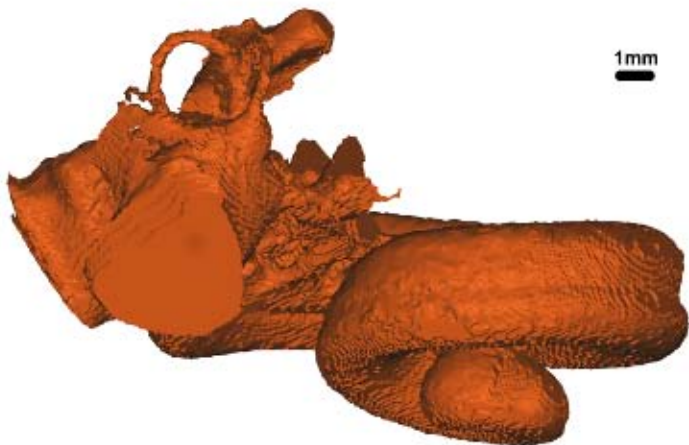
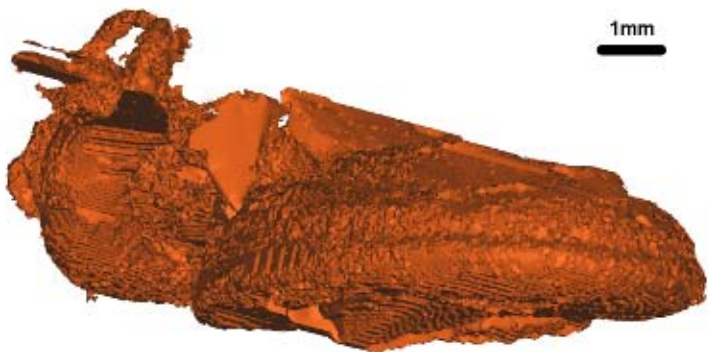
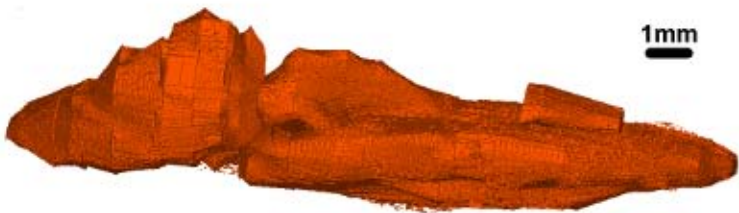
b

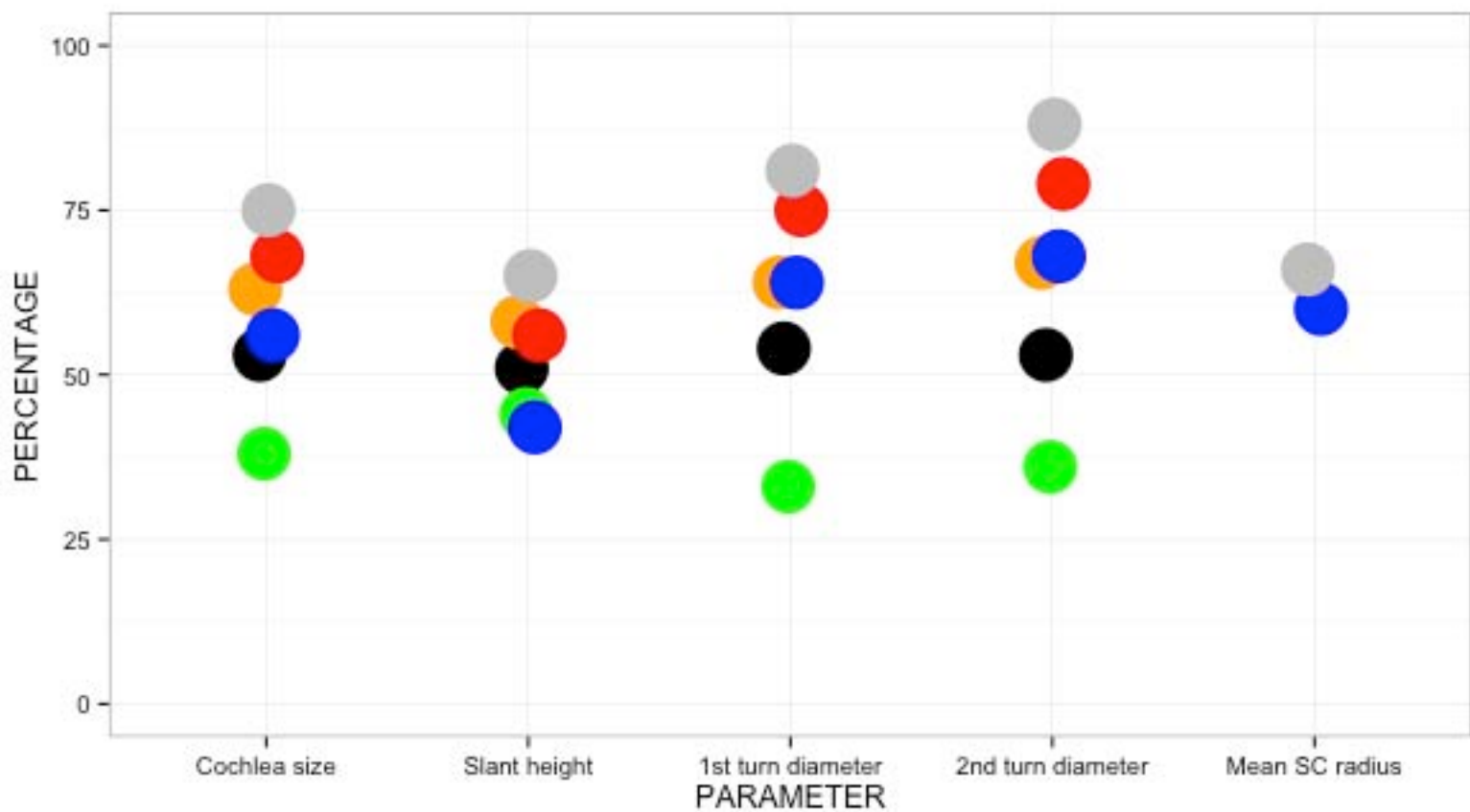


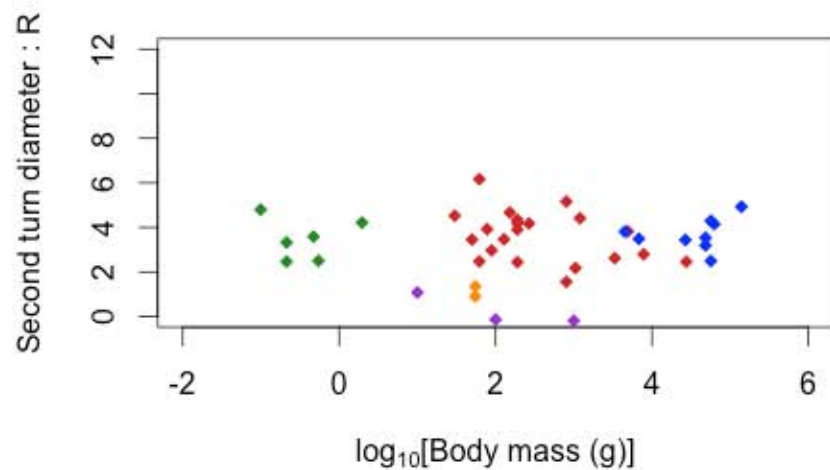
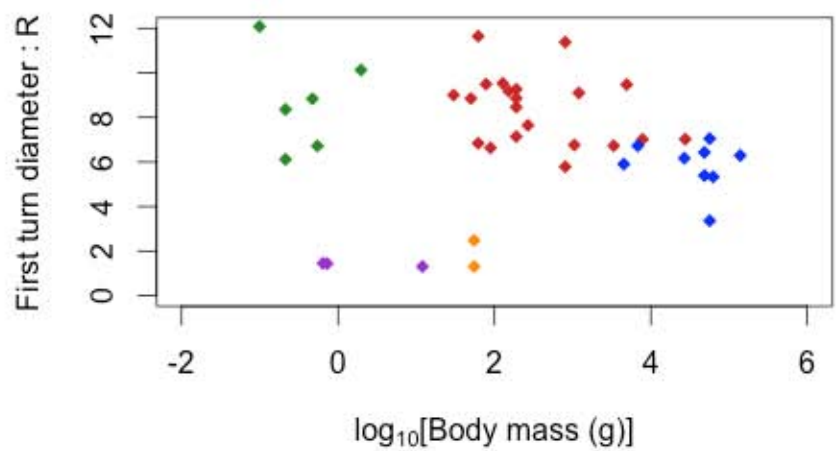
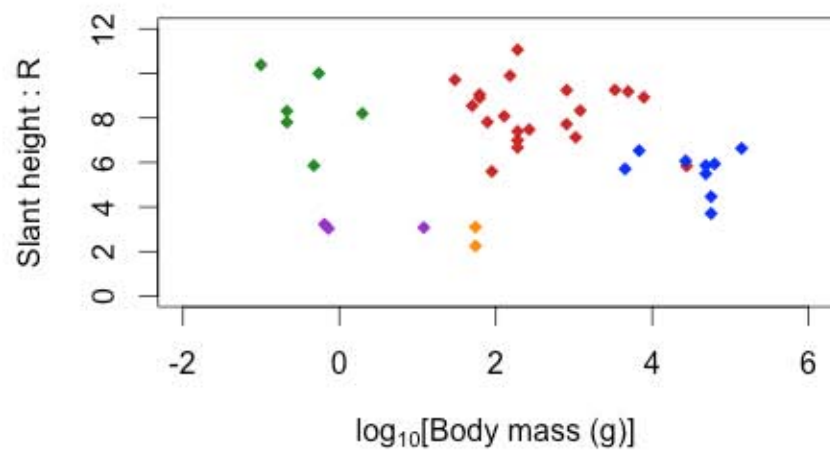
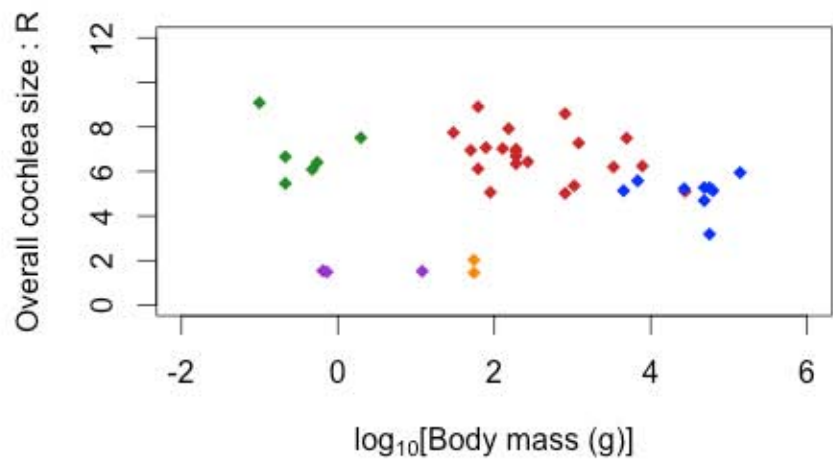
c



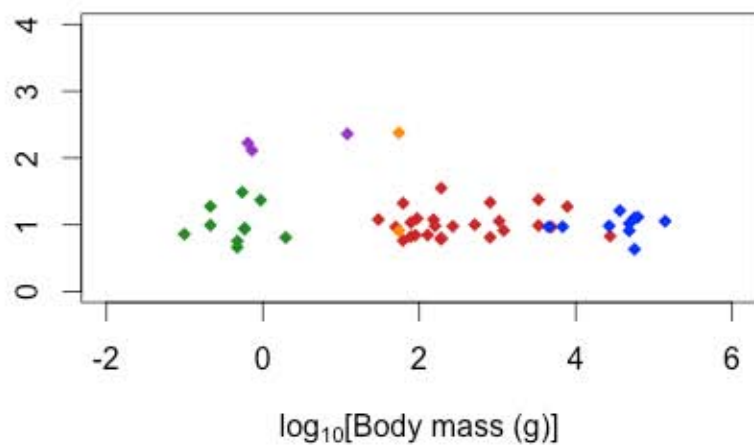
d



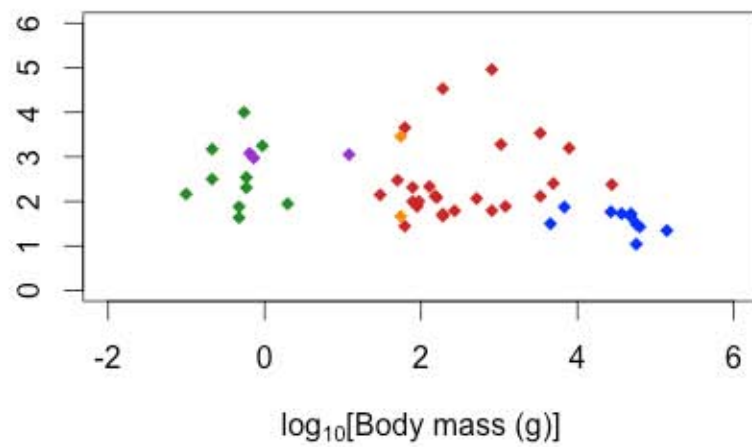




Slant height : First turn diameter



Slant height : Second turn diameter



First turn diameter : Second turn diameter

